



4

AD-A197 819

Technical Document 1306
July 1988

Electronic Properties and Current Carrying Capacity of High-Temperature Ceramic Superconductors

T. E. Jones
W. C. McGinnis
R. D. Boss
E. W. Jacobs
J. W. Schindler
C. D. Rees

DTIC
ELECTE
AUG 05 1988
H

UNCLASSIFIED

SECURITY CLASSIFICATION OF THIS PAGE

REPORT DOCUMENTATION PAGE

1a. REPORT SECURITY CLASSIFICATION UNCLASSIFIED			1b. RESTRICTIVE MARKINGS		
2a. SECURITY CLASSIFICATION AUTHORITY			3. DISTRIBUTION/AVAILABILITY OF REPORT		
2b. DECLASSIFICATION/DOWNGRADING SCHEDULE			Approved for public release; distribution is unlimited.		
4. PERFORMING ORGANIZATION REPORT NUMBER(S) NOSC TD 1306			5. MONITORING ORGANIZATION REPORT NUMBER(S)		
6a. NAME OF PERFORMING ORGANIZATION Naval Ocean Systems Center		6b. OFFICE SYMBOL (if applicable) NOSC 633	7a. NAME OF MONITORING ORGANIZATION		
6c. ADDRESS (City, State and ZIP Code) San Diego, California 92152-5000			7b. ADDRESS (City, State and ZIP Code)		
8a. NAME OF FUNDING/SPONSORING ORGANIZATION Office of Chief of Naval Research		8b. OFFICE SYMBOL (if applicable) OCNR-10P	9. PROCUREMENT INSTRUMENT IDENTIFICATION NUMBER		
8c. ADDRESS (City, State and ZIP Code) Arlington, VA 22217-5000			10. SOURCE OF FUNDING NUMBERS		
			PROGRAM ELEMENT NO. 61152N	PROJECT NO. ZT86	TASK NO. AGENCY ACCESSION NO. DN308 045
11. TITLE (include Security Classification) ELECTRONIC PROPERTIES AND CURRENT CARRYING CAPACITY OF HIGH-TEMPERATURE CERAMIC SUPERCONDUCTORS					
12. PERSONAL AUTHOR(S) T.E. Jones, W.C. McGinnis, R.D. Boss, E.W. Jacobs, J.W. Schindler, C.D. Rees					
13a. TYPE OF REPORT Final		13b. TIME COVERED FROM TO		14. DATE OF REPORT (Year, Month, Day) July 1988	
				15. PAGE COUNT 13	
16. SUPPLEMENTARY NOTATION					
17. COSATI CODES			18. SUBJECT TERMS (Continue on reverse if necessary and identify by block number)		
FIELD	GROUP	SUB-GROUP	ceramic superconductors bismuth-based superconductors holelike carriers		
19. ABSTRACT (Continue on reverse if necessary and identify by block number) Samples of both the $\text{YBa}_2\text{Cu}_3\text{O}_7$ family of high-temperature ceramic superconductor and the layered set of bismuth-based superconductors, described by the set of crystal structures $\text{Bi}_2\text{Sr}_2\text{Ca}_{n-1}\text{Cu}_n\text{O}_{2n+4+\delta}$, were synthesized and characterized by x-ray diffraction, and temperature-dependent resistivity and thermoelectric power measurements. Superconductivity in the yttrium-based materials is relatively insensitive to rare-earth substitutions for the yttrium. Critical current measurements on these materials reveal two characteristic critical current values. The intrinsic critical current, determined by the suppression of the transition midpoint, is estimated to be greater than 10^4 A/cm^2 at 77K. The critical current defined by the $R=0$ point is much less in bulk ceramics and limited by intercrystalline weak links. For the bismuth-based materials, two high-temperature superconducting phases have been observed with transition temperatures near 80 K and 110 K. Evidence from thermoelectric power measurements is presented which shows both electronlike and holelike carriers contribute to the electrical transport in this family of ceramic superconductors. However, all of the superconducting transitions observed involve holelike states.					
20. DISTRIBUTION/AVAILABILITY OF ABSTRACT <input type="checkbox"/> UNCLASSIFIED/UNLIMITED <input checked="" type="checkbox"/> SAME AS RPT <input type="checkbox"/> DTIC USERS			21. ABSTRACT SECURITY CLASSIFICATION UNCLASSIFIED		
22a. NAME OF RESPONSIBLE PERSON T.E. Jones			22b. TELEPHONE (include Area Code) 619-553-1594		22c. OFFICE SYMBOL Code 633

ELECTRONIC PROPERTIES AND CURRENT CARRYING CAPACITY OF HIGH-TEMPERATURE CERAMIC SUPERCONDUCTORS

F.E. Jones, W.C. McGinnis, R.D. Boss, E.W. Jacobs,
J.W. Schindler, and C.D. Rees
Naval Ocean Systems Center
San Diego, California

ABSTRACT

Samples of both the $\text{YBa}_2\text{Cu}_3\text{O}_7$ family of high-temperature ceramic superconductor and the layered set of bismuth-based superconductors, described by the set of crystal structures $\text{Bi}_2\text{Sr}_2\text{Ca}_{n-1}\text{Cu}_n\text{O}_{2n+4+\delta}$, were synthesized and characterized by x-ray diffraction, and temperature-dependent resistivity and thermoelectric-power measurements. Superconductivity in the yttrium-based materials is relatively insensitive to rare-earth substitutions for the yttrium. Critical current measurements on these materials reveal two characteristic critical current values. The intrinsic critical current, determined by the suppression of the transition midpoint, is estimated to be greater than 10^4 A cm^{-2} at 77 K. The critical current defined by the $R = 0$ point is much less in bulk ceramics and limited by intercrystalline weak links. For the bismuth-based materials, two high-temperature superconducting phases have been observed with transition temperatures near 80 K and 110 K. Evidence from thermoelectric power measurements is presented which shows that both electronlike and holelike carriers contribute to the electrical transport in this family of ceramic superconductors. However, all of the superconducting transitions observed involve holelike states.

INTRODUCTION

The report by Bednorz and Müller¹ of superconductivity above 30 K in La_2CuO_4 doped with barium or strontium has led superconductivity research into new directions. After having reached a mature level with A15 phase materials with superconducting transitions up to 23 K, interest in this field waned due to the extreme cryogenic environment required to achieve the superconducting state. Within a few months of the 30 K report, yet another high-temperature superconductor was announced with a superconducting critical temperature, T_c , above 90 K.² This material, shortly thereafter identified as $\text{YBa}_2\text{Cu}_3\text{O}_7$,³ superconducted well above the temperature of liquid nitrogen, 77 K. The 30 K lanthanum material forms in the perovskitelike K_2NiF_4 crystal structure.⁴ Numerous other materials are known to exist in this structure. Most are insulating and none were previously found to be superconducting. The 90 K yttrium superconductor, however, has an entirely new crystal structure not previously seen in nature. One striking feature of both the 30 K lanthanum and 90 K yttrium materials are planes of copper and oxygen (Cu-O). In addition, the yttrium material has a unique feature - chains of copper and oxygen - in one direction in the orthorhombically distorted basal plane.⁵ Some researchers have ascribed some significance to the Cu-O chain structure as being important for high-temperature superconductivity.

Most applications of superconductivity require the ability to carry a large amount of current. Current densities on the order of 10^5 – 10^6 A cm^{-2} , are desired for most applications, both in microelectronics and large-scale high-current high-power applications such as the generation of large magnetic fields and energy storage. This paper reports preliminary measurements of the current carrying capacity of bulk ceramics in these two families of materials using pulsed transport techniques.

The discovery of superconductivity above 90 K has spurred intense theoretical interest in the possible mechanisms responsible. In conventional superconductors, studied since the original discovery of superconductivity in 1911,⁶ phonons (lattice vibrations) provide a net attractive interaction among conduction electrons in a narrow range of energy near the Fermi surface. This attractive interaction allows electron pairs to form and results in a macroscopic quantum state. One consequence of this lower energy condensed state is zero resistance. There are many other properties of superconductors besides zero resistance.⁷ The formal explanation of superconductivity, from a microscopic quantum-mechanical point of view, was due to the Bardeen, Cooper, and Schrieffer (BCS) theory, published in 1957, for which they were later awarded the Nobel Prize. Although numerous other mechanisms of superconductivity have been suggested over the years, the BCS theory based on the electron-phonon interaction, is the only one accepted as valid. No material has yet been found in which superconductivity can be attributed to any other mechanism. However, the very high critical temperatures routinely achieved today with the new ceramics has led theorists to question the applicability of the old theory and to offer alternatives.⁸

Less than a year after the discovery of 90 K superconductivity, two new families of materials have been discovered based on bismuth^{9,10} and thallium.^{11,12} These new discoveries created a great interest in the electronic states of the materials and, in particular, the charge transfer to and from the Cu-O planes vis-a-vis the $\text{YBa}_2\text{Cu}_3\text{O}_7$ family. With no Cu-O chains in the bismuth and thallium materials,¹³ the role of the Bi-O and Tl-O planes is being investigated. One technique described in this paper involves the measurement of the absolute thermoelectric power (thermopower) versus temperature. The thermopower of a material generally yields the sign of the dominant charge carrier and, as in Hall effect measurements, distinguishes between electron (n-type carriers) and hole (p-type carriers) conduction. In the first high-temperature superconductors, $(\text{La,Sr})_2\text{CuO}_4$ and $\text{YBa}_2\text{Cu}_3\text{O}_7$, both the normal state conductivity and the superconductivity have been shown to be due to holelike states.^{14,15} In the lanthanum material, doping with a divalent element, barium or strontium, in place of the trivalent lanthanum, effectively removes electrons from the Cu-O planes leaving conducting holes.

Also, x-ray photoemission spectroscopy^{16,17} shows that doping creates holes in the Cu-O planes. However, in the heavily doped lanthanum material (25-percent strontium replacement), evidence from thermoelectric power measurements extended above room temperature have been reported which suggest that there is also a contribution to the normal conductivity from electrons.¹⁸ In the yttrium material, empirical atom-atom potential calculations,¹⁹ extended Huckel molecular orbital calculations,²⁰ and bond-valence calculations²¹ imply electron transfer from the Cu-O planes to the Cu-O chains. In addition, the results of substitutional studies with zinc and gallium by Xiau et al.²² show that it is the Cu-O planes which are important for superconductivity, rather than the Cu-O chains, in $\text{YBa}_2\text{Cu}_3\text{O}_7$.

In the bismuth family of materials, one could argue that electrons might be transferred from the Bi-O planes to the Cu-O planes. Because bismuth presumably goes into the material in the valence +3 state, partial conversion to bismuth +5 would require hole states on the bismuth planes and electron states on the Cu-O planes. If such electron transfer occurs and the charge carriers in these materials reside on the Cu-O planes (as in the other copper-oxide superconductors), then conduction would be due to n-type electronic states. This would be quite different than in the other copper oxide high-temperature superconducting ceramics, where the superconductivity comes from paired hole states. On the other hand, band structure calculations of Hybertsen and Mattheiss indicate that the Bi-O planes in effect dope the Cu-O planes with additional holes (i.e., that electrons are transferred from the Cu-O planes to the Bi-O planes).²³ Assuming these band-structure calculations are correct, there may be an n-type contribution to the conductivity from the Bi-O planes, but the superconductivity would be due to the pairing of holes in the Cu-O planes as observed in all other copper-oxide superconducting ceramics to date.

For the new class of bismuth-based materials described by the formula $\text{Bi}_2\text{Sr}_2\text{Ca}_{n-1}\text{Cu}_n\text{O}_{2n+4+\delta}$, one would like to know the origin of the charge carriers, whether they are electrons or holes, and which carriers condense into the superconducting phases at high temperature. The results of thermoelectric power measurements on several samples in the bismuth family are presented which will provide answers to some of these questions.

EXPERIMENTAL TECHNIQUES

All samples were prepared by solid-state reaction of the constituent oxides and/or carbonates. High-purity fine powders of the starting materials (obtained from Aesar), were mixed in the desired molar ratio, placed in porcelain or alumina crucibles, and calcined (heated in a furnace to reduce any of the carbonates to oxides) for several hours. The samples were then ground with a mortar and pestle to a fine powder. The calcining/grinding procedure was repeated more than once for some samples. At the end of the calcining cycle(s), the samples were ground to a powder and pressed into small pellets at a pressure of several thousand pounds per square inch. The pellets were placed on alumina disks for the final processing cycle in the furnace. The furnace atmosphere, either oxygen or air, as well as the temperature settings and cycle times used, were sample dependent. These and other details of sample preparation are described in the next section.

The electrical resistance R of the samples was measured with small dc currents (typically 10 mA) using a four-probe technique to eliminate the effects of contact resistance. Wires were soldered to the samples with indium. The sample voltage was taken to be the average of the difference in values obtained for plus and minus currents. In this way, the contribution of small, unavoidable thermoelectric voltages is cancelled out. These voltages arise from junctions between two different materials in the measuring circuit in the presence of a temperature gradient. They exist even at zero current, and do not change when the current is switched. This precaution is particularly important when the samples are superconducting. With no switching of the current, a sample with $R = 0$ will otherwise appear to have a small, non-zero resistance (the parasitic thermoelectric voltage divided by the current).

The resistance measurements, as well as the critical current measurements described below, were performed with the samples in good thermal contact with a copper stage on the cold-head of a closed-cycle He-4 refrigerator. In some cases, the temperature-dependent sample resistance was measured with the sample mounted on a copper sample stage which could be cooled to 77 K by dipping in liquid nitrogen. This "dip probe" was then withdrawn from the liquid and allowed to slowly warm to room temperature. In either case, the stage (sample) temperature was monitored with a calibrated silicon diode.

For a given temperature below T_c , a superconductor will have zero resistance only for current densities less than the so-called critical current density, $J_c(T)$. As indicated, J_c is temperature dependent, being smallest when the sample is near its critical temperature, and increases as the temperature is lowered. The method used here for measuring the critical current density is a variation on the dc, four-probe technique used to measure the sample resistance. In both cases, a given current I is applied to the sample, and the sample voltage V (related to the sample resistance by Ohm's law $V = IR$) is measured as the sample slowly warms through the superconducting transition. Direct measurement of the critical current of bulk samples usually requires substantially larger currents than would be used in a simple resistance measurement. This fact introduces two complications which dictate some changes in the experimental arrangement: sample heating and equipment limitations on the maximum available current.

Since the quantity of interest is the critical current density, the second problem can be minimized by reducing the sample cross section to as small an area as physically possible. This was accomplished by cutting a slot between the current (and voltage) contacts on the sample, leaving a small bridge between the two sides of the sample.²⁴ This bridge forms a "weak link" with respect to the sample's current carrying capability.

Ohmic heating of the sample by the applied current can raise the sample temperature with respect to that of the measuring thermometer (the diode attached to the sample stage). Since J_c decreases with increasing temperature, this effect results in a critical current density that is smaller than the value that would be measured if the sample were at the same temperature as the thermometer. The highest resistance (and, therefore, the greatest source of heat) is usually at the point of contact between the current-carrying wires and the sample. Thus, sample heating can be reduced by making the contact resistance as small as possible. Total contact resistances on the order of 75 to 100 m Ω were achieved by applying silver paint (Dupont 4949TM) to the samples and heating to a temperature of about 850 C.²⁵

Another way to avoid sample heating is to reduce the amount of time that current is actually flowing in the sample. A pulsed technique, which employs low-frequency current pulses applied at a low duty cycle, is illustrated schematically in Fig. 1. A box-car averager measures the sample voltage by performing a weighted average over 25 to 50 pulses, giving a better signal-to-noise ratio than is possible with single pulse measurements. The duty cycle (pulse width divided by the time between pulses) was chosen such that doubling the pulse width gave no measureable change in the resistance versus temperature characteristics of the sample.

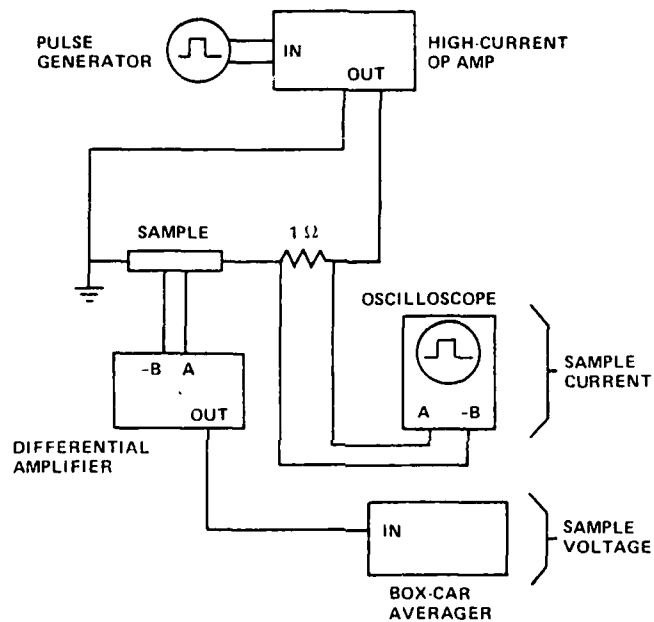


Fig. 1. Pulsed Current Technique for the Measurement of Critical Current.

Another way in which the samples were characterized was by measurement of their absolute thermoelectric power. To measure the thermopower, a temperature gradient ΔT is produced across an electrically isolated sample giving rise to a thermoelectric voltage ΔV across the sample. The thermoelectric power S (or Seebeck coefficient) is given by $\Delta V / \Delta T$ (as $\Delta T \rightarrow 0$). The thermopower data reported below were obtained using a slow ac differential technique.²⁶ A small, slowly oscillating thermal gradient was produced by alternately heating two parallel quartz blocks which were bridged by the samples. A detailed description of the procedure can be found elsewhere.²⁷ The temperature difference ΔT between the blocks (that is, the temperature drop across the samples) was measured using a copper-constantan/copper differential thermocouple. The whole apparatus was mounted in a closed-cycle refrigerator in such a way that the thermopower and four-probe resistance of the samples could be measured during a single experimental run. Copper wires were used to measure the voltage difference ΔV across the sample. The ratio $\Delta V / \Delta T$ is then equal to the sample thermopower minus the thermopower of the copper voltage leads. The temperature-dependent thermopower of the copper voltage leads is, therefore, required in order to obtain the samples' absolute thermopower. For temperatures below the superconducting transition of a sample, the sample thermopower is zero. This fact enabled direct measurement of the voltage lead thermopower up to this temperature. Above the transition, literature values of S_{Cu} ,²⁸ corrected by the new thermopower scale of Roberts,²⁹ were used.

EXPERIMENTAL RESULTS

A number of samples of the $YBa_2Cu_3O_7$ family of high-temperature superconductors have been prepared. This class of superconductor was typically calcined in air at about 925 to 930°C. After pressing into pellets, they were placed in a furnace in flowing oxygen, sintered at 930 to 955°C for several hours, annealed at about 500°C for a few hours, and slowly cooled to 200°C.

A-1

Figure 2 shows plots of resistance (normalized to that at room temperature) versus temperature for the yttrium-based material, as well as for several of the rare-earth substituted analogs. They all exhibit sharp superconducting transitions between 91 and 95 K, indicating that the particular element R used in the $\text{RBa}_2\text{Cu}_3\text{O}_7$ structure plays no significant role in the superconductivity.

The temperature dependence of the thermopower and resistivity of another $\text{YBa}_2\text{Cu}_3\text{O}_7$ sample is presented in Fig. 3. Both sets of data show the superconducting transition at 94° K. The thermopower is positive above this temperature, indicating holelike carriers.

Figure 4 illustrates the effect of increasing current density on the resistive transition of a third $\text{YBa}_2\text{Cu}_3\text{O}_7$ sample. As seen in the figure, the temperature at which the biggest drop in resistance occurs changes very little as the current density is increased from 0.75 to 429 A cm^{-2} . The main effect is the development of a "tail" or "foot" in which the $R = 0$ point is pushed to successively lower temperatures with increasing current. The dual characteristic of the transition is likely due to the granular nature of this ceramic material. The sample consists of Josephson-coupled superconducting grains separated by grain boundaries or even non-superconducting, off-stoichiometry material. The large resistance drop can be associated with the superconducting transition within the individual grains. The sample does not go completely superconducting, however, until the temperature is low enough for Josephson tunneling between these superconducting grains. The temperature dependence of the $R = 0$ critical current density for this sample is shown in Fig. 5a, and can be interpreted in terms of the above tunneling model.³⁰ Figure 5b is described below.

Samples of the bismuth family of superconductors with various starting compositions and heat treatments have also been prepared and characterized. They were typically calcined in air at 860°C, ground, and pressed into pellets. The pellets were heated, again in air, at temperatures between 860 and 880°C for periods of time ranging from 65 to 158 hours, and slowly cooled to 200°C.

The resistive transitions for four of these samples are shown in Fig. 6. The presence of two distinct superconducting phases, with transition temperatures near 80 K and 110 K, is suggested by these plots. This is particularly true in the 4-3-3-6 sample (small dashes), which must contain substantial amounts of both phases.

Resistivity and thermopower data from another presumably mixed-phase bismuth-based sample are shown in Fig. 7. The two transitions are clearly seen in both properties. These data, and the resistivity data of Fig. 6, support the conclusion that these samples have the composition $\text{Bi}_2\text{Sr}_2\text{Ca}_{n-1}\text{Cu}_n\text{O}_{2n+4+\delta}$ with a mixture of the $n = 2$ and $n = 3$ phases, corresponding to the 80 K and 110 K transitions, respectively. Like the $\text{YBa}_2\text{Cu}_3\text{O}_7$ material, holes appear to be the dominant carrier, at least up to room temperature.

Critical current measurements on one of the low T_c bismuth-based samples were also made, and the temperature dependence of the $R = 0$ J_c is plotted in Fig. 5b. The difference in the exponents of the critical current density for the yttrium and bismuth materials is presently being investigated.

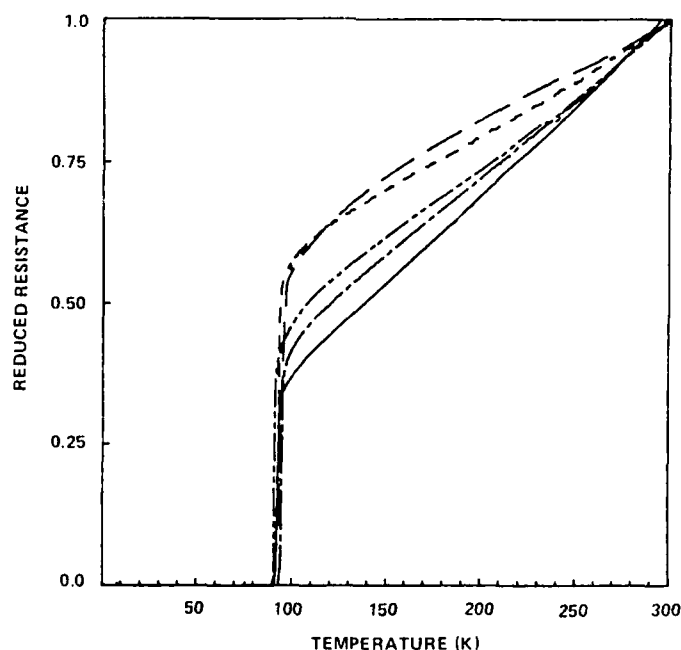


Fig. 2. Reduced Resistance Versus Temperature for $\text{RBa}_2\text{Cu}_3\text{O}_7$, for R = Y (Solid Line), Gd (Large Dashes), Dy (Small Dashes), Ho (Line with One Dash), and Yb (Line with Two Dashes).

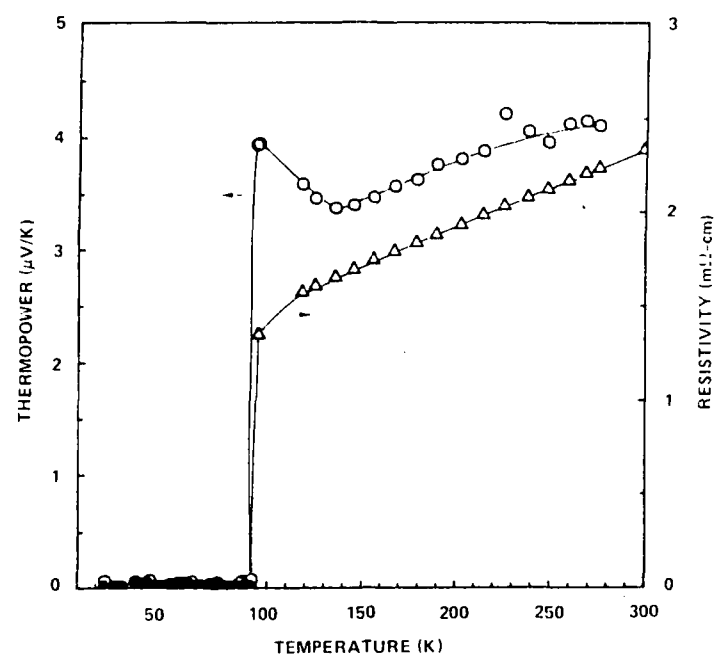


Fig. 3. Thermoelectric Power (O) and Resistivity (Δ) for a Sample of $\text{YBa}_2\text{Cu}_3\text{O}_7$.

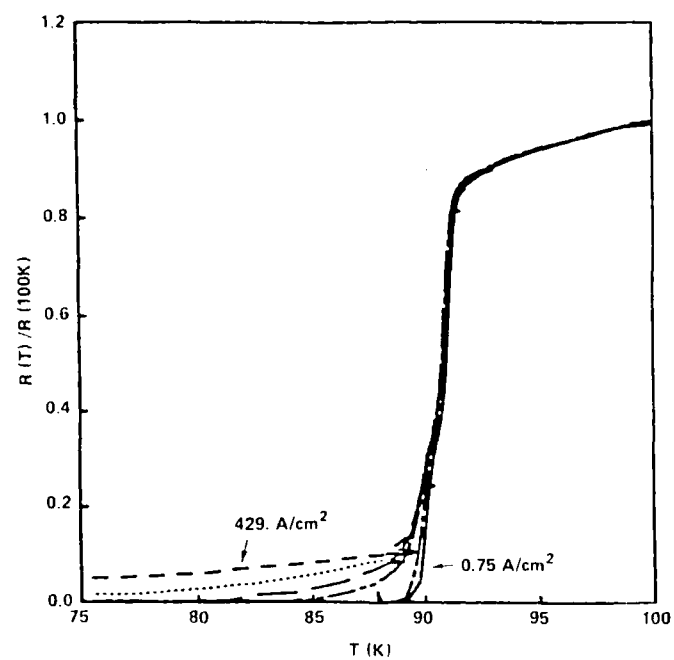


Fig. 4. Normalized Resistance, $R(T)/R(100\text{ K})$, Versus Temperature for a Sample of $\text{YBa}_2\text{Cu}_3\text{O}_7$ Measured with Different Current Densities.

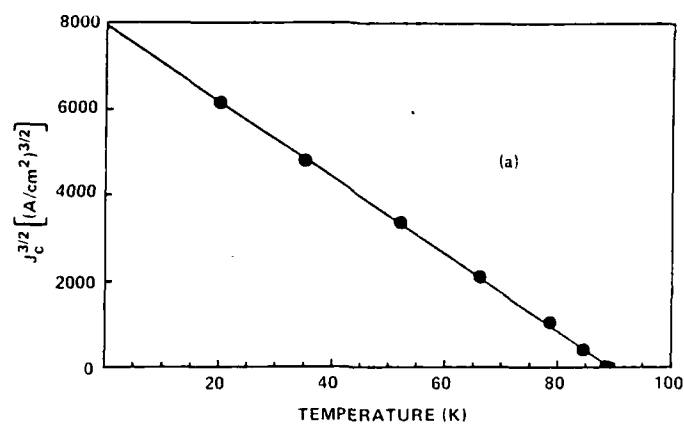


Fig. 5. (a) Critical Current Density J_c to the $3/2$ Power Versus Temperature at which $R = 0$ for a Sample of $YBa_2Cu_3O_7$.

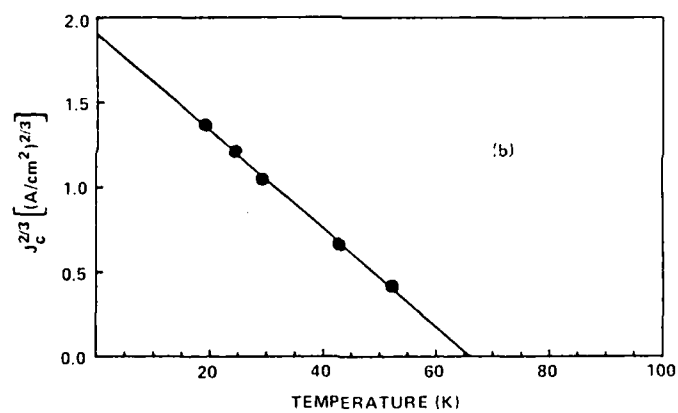


Fig. 5. (b) Critical Current Density J_c to the $2/3$ Power Versus Temperature at which $R = 0$ for a Sample of $Bi_2Sr_2CaCu_2O_x$.

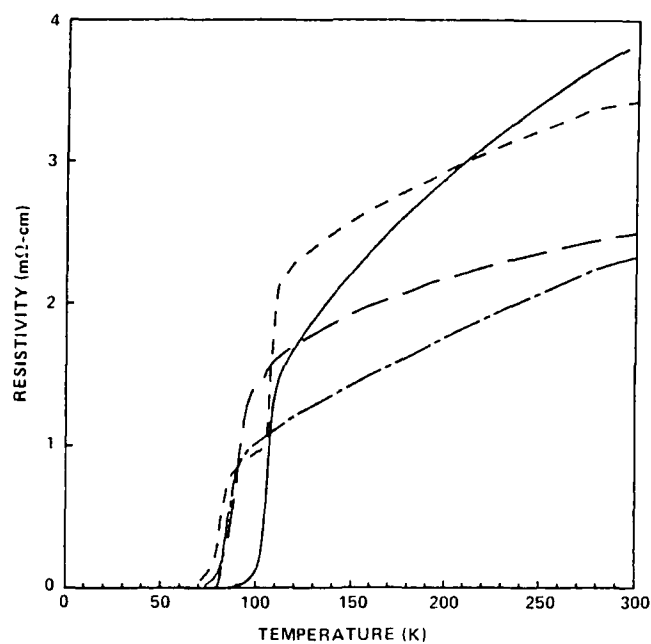


Fig. 6. Resistivity Versus Temperature for Four Bismuth-Based Superconductors of Nominal Bi:Sr:Ca:Cu Composition 4-3-3-6 (Solid Line), 4-3-3-6 (Small Dashes), 2-2-2-3 (Large Dashes), and 2-2-1-2 (Line with One Dash).

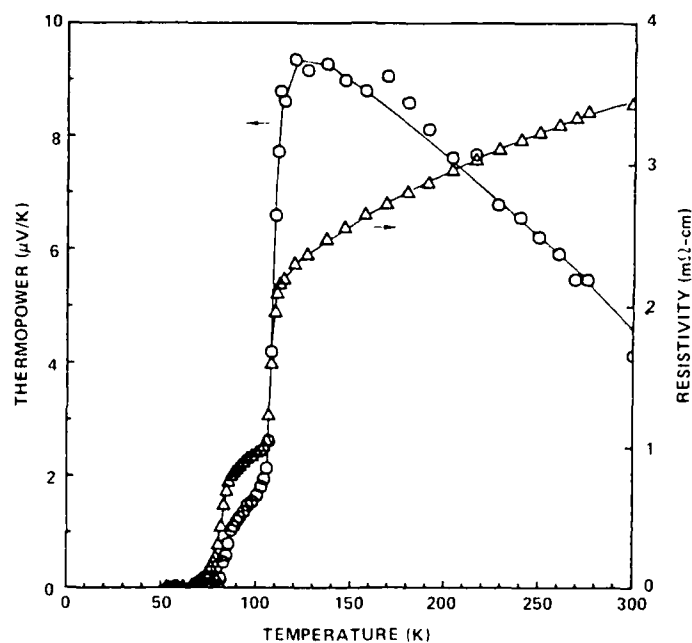


Fig. 7. Thermoelectric Power (○) and Resistivity (Δ) for a Bi-Sr-Ca-Cu-O Sample of Nominal Composition 4-3-3-6 Which Shows Both High-Temperature Transitions Seen in This System.

CONCLUSIONS

The results of critical current measurements on $\text{YBa}_2\text{Cu}_3\text{O}_7$ show that one can speak of two critical currents in these materials. One, the intrinsic critical current, determined by the midpoint of the transition, is estimated by extrapolation to be greater than 10^4 A cm^{-2} at 77 K. On the other hand, the weak-link critical current, as measured by the point of zero resistance, appears to be limited by intercrystalline boundaries and/or nonsuperconducting regions in the material. Since thin, oriented films have demonstrated large intrinsic critical currents, the current carrying capacity of these ceramics can be large. The technological issue is whether these materials can be produced in bulk ceramic form in such a way as to eliminate the weak links.

Additionally, we have presented conclusive evidence that the two high-temperature superconductive transitions, near 80 K and 110 K, in the $\text{Bi}_2\text{Sr}_2\text{Ca}_{n-1}\text{Cu}_n\text{O}_{2n+4+\delta}$ family of superconductors are due to holelike states, as is the case with all other high-temperature copper-oxide superconductors discovered to date. The p-type carriers most likely arise from electron charge transferred from the Cu-O planes to the Bi-O interplanar regions, perhaps to extra oxygen sites which are partially occupied. Further, even though holes dominate the electrical transport, we have presented evidence that electrons, as well as holes, contribute to the normal state conductivity in this new class of layered materials.

REFERENCES AND NOTES

1. Bednorz, J.G. and K.A. Müller, *Z. Phys. B Condensed Matter*, vol. 64, p. 189, 1986.
2. Wu, M.K., J.R. Ashburn, C.J. Torng, P.H. Hor, R.L. Meng, L. Gao, Z.J. Huang, Y.Q. Wang, and C.W. Chu, *Phys. Rev. Lett.*, vol. 58 (9), p. 908, 1987.
3. Cava, R.J., B. Batlogg, R.B. van Dover, D.W. Murphy, S. Sunshine, T. Siegrist, J.P. Remeika, E.A. Rietman, S. Zahurak, and G.P. Espinosa, *Phys. Rev. Lett.*, vol. 58 (16), p. 1676, 1987.
4. Takagi, H., S. Uchida, K. Kitazawa, and S. Tanaka, *Jpn. J. Appl. Phys. Lett.*, vol. 26, L1, 1987.
5. Grant, P.M., R.B. Beyers, E.M. Engler, G. Lim, S.S.P. Parkin, M.L. Ramirez, V.Y. Lee, A. Nazzari, J.E. Vazquez, and R.J. Savoy, *Phys. Rev. B*, vol. 35, p. 7242, 1987.
6. Kamerlingh Onnes, H., *Akad. van Wetenschappen* (Amsterdam) vol. 14, 113, p. 818, 1911.
7. Kittel, C., *Introduction to Solid State Physics*, 4th ed., 1971, John Wiley & Sons, Inc., New York.
8. Hirsch, J.E., *Phys. Rev. Lett.*, vol. 59 (2), p. 228, 1987.
9. Chu, C.W., J. Bechtold, L. Gao, P.H. Hor, Z.J. Huang, R.L. Meng, Y.Y. Sun, Y.Q. Wang, and Y.Y. Xue, *Phys. Rev. Lett.*, vol. 60 (10), p. 941 (1987).
10. Takayama-Muromachi, E., Y. Uchida, A. Ono, F. Iruki, M. Onoda, Y. Matsui, K. Kosuda, S. Takakawa, and K. Kato, preprint submitted to *Jpn. J. Appl. Phys.*
11. Sheng, Z.Z., A.M. Hermann, A. El Ali, C. Almasan, J. Estrada, T. Datta, and R.J. Matson, *Phys. Rev. Lett.*, vol. 60 (10), p. 937, 1988.
12. Hazen, R.M., L.W. Finger, R.J. Angel, C.T. Prewitt, N.L. Ross, C.G. Hadjidakos, P.J. Heaney, D.R. Veblen, Z.Z. Sheng, A. El Ali, and A.M. Hermann, *Phys. Rev. Lett.*, vol. 60 (16), p. 1657, 1988.
13. Tarascon, J.M., Y. LePage, P. Barboux, B.G. Bagley, L.H. Greene, W.R. McKinnon, G.W. Hull, M. Giroud, and D.M. Hwang, submitted to *Phys. Rev.*
14. Uher, C., A.B. Kaiser, K.E. Gmelin, and L. Walz, *Phys. Rev. B*, vol. 36 (10), p. 5676, 1987.
15. Uher, C., A.B. Kaiser, *Phys. Rev. B*, vol. 36 (10), p. 5680, 1987.
16. Tranquada, J.M., *Phys. Rev. B*, vol. 36, p. 5263, 1987.
17. Shen, Z.X., J.W. Allen, J.J. Yen, J.S. Kang, W. Ellis, W. Spicer, I. Lindau, M.B. Maple, Y.D. Dalichaouch, M.S. Torikachvili, J.Z. Sun, and T.H. Geballe, *Phys. Rev. B*, vol. 36, p. 8414, 1987.
18. Michel Evain, Myung-Hwan Whangbo, Mark A. Beno, and Jack M. Williams, *J. Am. Chem. Soc.*, vol. 110, p. 614, 1988.
19. Whangbo, M.H., Michel Evain, Mark A. Beno, Urs Geiser, and Jack M. Williams, *Inorg. Chem.*, vol. 27, p. 467, 1988.
20. Curtiss, L.A., T.O. Brun, and D.M. Gruen, *Inorg. Chem.*, 27, p. 1421, 1988.
21. O'Keeffe, M. and S. Hensen, *J. Am. Chem. Soc.*, 110, p. 1506, 1988.
22. Xiao, G., M.Z. Cieplak, A. Gavrin, F.H. Streitz, A. Bakhshai, and C.L. Chien, *Phys. Rev. Lett.*, vol. 60 (14), p. 1446, 1988.
23. Hybertsen, M.S. and L.F. Mattheiss, *Phys. Rev. Lett.*, vol. 60 (16), p. 1661, 1988.
24. Higashino, Y., T. Takahashi, T. Kawai, and S. Naito, *Jpn. J. Appl. Phys.*, vol. 26, p. L1211, 1987.
25. van der Maas, J., V.A. Gasparov, and D. Pavuna, *Nature*, vol. 328, p. 603, 1987.
26. Chaikin, P.M. and J.F. Kwak, *Rev. Sci. Instrum.*, vol. 46 (2), p. 218, 1975.
27. Jones, T.E., W.C. McGinnis, R.D. Boss, E.W. Jacobs, J.W. Schindler, and C.D. Rees, submitted to the American Chemical Society for inclusion in *Physical Chemistry of High Temperature Superconductors*.
28. Crisp, R.S., W.G. Henry, and P.A. Schroeder, *Philos. Mag.*, vol. 10, p. 553, 1964.
29. R.B. Roberts, *Philos. Mag.*, vol. 36 (1), p. 91, 1977.
30. Ambegaokar, V. and Alexis Baratoff, *Phys. Rev. Lett.*, vol. 10 (11), p. 486, 1963.

END

DATE

FILMED

DTIC

9-88